

# Continuous Symmetry Analysis of Tetrahedral/Planar Distortions. Copper Chlorides and Other AB<sub>4</sub> Species

Shahar Keinan and David Avnir\*

Institute of Chemistry and The Lise Meitner Minerva Center for Computational Quantum Chemistry, The Hebrew University of Jerusalem, Jerusalem 91904, Israel

Received June 22, 2000

The symmetry of tetracoordinated copper complexes, especially of CuCl<sub>4</sub><sup>2-</sup>, is analyzed in terms of quantitative continuous symmetry. These complexes acquire structures that span from tetrahedral to planar, with all gradual variations in between, a property that is evaluated here in terms of their degrees of tetrahedrality ( $S(T_d)$ ) and square planarity ( $S(D_{4h})$ ). It was found that out of the large arsenal of geometry-allowed tetrahedral structures, each of which is characterized by specific  $S(T_d)$  and  $S(D_{4h})$  pair values, copper complexes concentrate on an extremely well-defined correlation line linking these two symmetry-content measures; that is, only very specific pairs of  $S(T_d)$  and  $S(D_{4h})$  values that dictate each other are allowed. Furthermore, it was found that of the various routes that can lead from a tetrahedron to a planar square, the mode known as spread fits exactly in its symmetry  $S(T_d)/S(D_{4h})$  characteristics the observed symmetry behavior of the copper complexes. Interestingly, the spread mode reflects also the (nearly) minimal possible values of  $S(T_d)/S(D_{4h})$  pairs, namely, the minimal symmetry-distortive route. Hints that this symmetry correlation line reflects universal features that go beyond copper are provided by the symmetry-content analysis of Ni and Pt complexes, of various Zn complexes within a metalloprotein and even of CC<sub>4</sub> fragments, all of which obey the same line. A new potential-energy surface is introduced, the axes of which are  $S(T_d)$ ,  $S(D_{4h})$ , and the energy. Calculating this surface for CuCl<sub>4</sub><sup>2-</sup> reveals an important result: The minimal molecular symmetry distortive spread correlation line coincides with the (only) energy valley of the map. Symmetry and energy are intimately related in their drive to minimal values.

## 1. Background

**Tetrahedral to Planar Molecular Distortions.** At the dawn of modern stereochemistry, Van't Hoff<sup>1</sup> and Le Bel<sup>2</sup> independently reached a paradigm-shift insight, which raised the tetrasubstituted carbon from its two-dimensional (2D) flat floor to the three-dimensional (3D) rich world of structures. As is typical of such revolutionary steps, the conceptual jump was sharp, from 2D square planarity to 3D tetrahedrality with no "in-betweens". Such intermediate-geometry structures have been introduced during the following years, when the ongoing accumulation of structural data on tetrasubstituted and tetracoordinated AB<sub>4</sub> molecules took place.<sup>3</sup> The collected voluminous data have indeed revealed that while perfect square planarity (C<sub>4</sub> symmetry in 2D or D<sub>4h</sub> (AB<sub>4</sub>) symmetry in 3D) and perfect tetrahedrality (T<sub>d</sub>) were found, more common are AB<sub>4</sub> molecules with structures that deviate from these ideal extremes to the extent that a decision on which of the ideal references they resemble is not always straightforward.<sup>4</sup> Because the AB<sub>4</sub> molecule is the most elementary building block in chemistry that introduces three-dimensionally, the problem of quantifying the description of the shape of AB<sub>4</sub> has received a major effort. This quantification has been based on the use of specific

geometry parameters (angles, bond lengths), with a classical example being the works of Muetterties et al.<sup>5</sup> and Halvorson et al.,<sup>6</sup> and the use of symmetry coordinates by Burgi, Dunitz, et al.<sup>7</sup> (implemented in ref 8), where plenty of structural correlations have been identified<sup>9</sup> and a proposition made of an inherent link between static data and chemical dynamics.<sup>10</sup>

The quantification of the description of the shapes of AB<sub>4</sub> molecules is particularly needed for the search of correlations between shape and chemical, physical, and biochemical parameters. Such correlations have been the focus of our research in recent years, by proposing to treat symmetry (and chirality) as a measurable continuous structural property.<sup>11</sup> Using this approach, we indeed identified quantitative correlations with symmetry/chirality in many domains of chemistry. Examples include a correlation between the degree of centrosymmetry and hyperpolarizability,<sup>12</sup> the application of the degree of centrosymmetry as a detector of melting points in small

\* To whom correspondence should be addressed. E-mail: david@chem.ch.huji.ac.il.

- (1) Van't Hoff, J. H. *Arch. Neerl. Sci. Exactes Nat.* **1874**, 9, 445–454. English translation: Van't Hoff, J. H. *Classics in the Theory of Chemical Combination*; Benfey, O. T., Ed.; Dover: New York, 1963; Vol. 1.
- (2) Le Bel, J. A. *Bull. Chim. Soc. Fr.* **1874**, 22, 337–347. English translation: Le Bel, J. A. *Classics in the Theory of Chemical Combination*; Benfey, O. T., Ed.; Dover: New York, 1963; Vol. 1.
- (3) Favas, M. C.; Kepert, D. L. *Prog. Inorg. Chem.* **1980**, 27, 325–449.
- (4) Gillespie, R. J. *Coord. Chem. Rev.* **2000**, 197, 51–69.

- (5) Muetterties, E. L.; Guggenberger, L. J. *J. Am. Chem. Soc.* **1974**, 96, 1748–1756.
- (6) Halvorson, K. E.; Patterson, C.; Willett, R. D. *Acta Crystallogr.* **1990**, B46, 508–519.
- (7) (a) Murray-Rust, P.; Burgi, H.-B.; Dunitz, J. D. *J. Am. Chem. Soc.* **1975**, 97, 921–922. (b) Murray-Rust, P.; Burgi, H.-B.; Dunitz, J. D. *Acta Crystallogr.* **1978**, B34, 1793–1803.
- (8) Cammi, R. *Comput. Chem.* **1994**, 18, 405.
- (9) (a) Burgi, H.-B.; Dunitz, J. D. *Structure Correlation*; Burgi, H.-B., Dunitz, J. D., Eds.; VCH: Weinheim, 1994; Vol. 1, pp 163–204. (b) Auf der Heyde, T. *Structure Correlation*; Burgi, H.-B., Dunitz, J. D., Eds.; VCH: Weinheim, 1994; Vol. 1, pp 337–368.
- (10) Burgi, H.-B.; Dunitz, J. D. *Acc. Chem. Res.* **1983**, 16, 153–161.
- (11) Avnir, D.; Katzenelson, O.; Keinan, S.; Pinsky, M.; Pinto, Y.; Salomon, Y.; Zabrodsky Hel-Or, H. *The Measurement of Symmetry and Chirality: Conceptual Aspects*; Rouvray, D. H., Ed.; Research Studies Press: Taunton, England, 1997; pp 283–324.

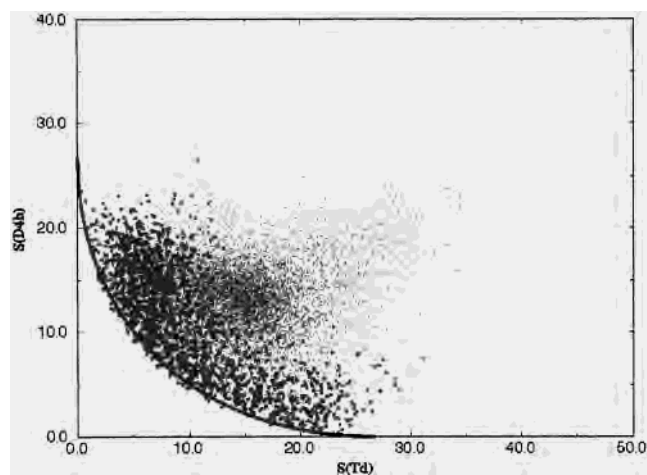


**Figure 1.** Degree of square planarity  $S(D_{4h})$  vs the degree of tetrahedrality  $S(T_d)$  of 12 000 randomly created tetrahedra (all dots). A subgroup of 2000 random tetrahedra restricted by bond angles not smaller than  $60^\circ$  are shown as well (black circles). Out of this cloud of possible tetracoordinated structures, copper complexes follow only the superimposed black line.

clusters,<sup>13</sup> energy/chirality correlations in the enantiomerization of chiral fullerenes,<sup>14</sup> a correlation between chirality of enzyme inhibitors and their efficiency of reaction with active sites,<sup>15</sup> and structure–activity correlations of HIV protease inhibitors dictated by quantitative  $C_2$  symmetry.<sup>16</sup>

In this report, the first of two parts, we concentrate on a central class of  $AB_4$  molecules exhibiting the full range of tetrahedral to planar distortions,<sup>6</sup> namely, on tetracoordinated Cu complexes in general and on the halides in particular. In this first part we analyze the continuous symmetry behavior of the complexes and its relation to their underlying energetics. In the following second part we identify correlations between the degree of tetrahedrality or square planarity and various spectroscopic properties. The continuous symmetry measure (CSM) approach we employ for the analysis of the molecular distortion of copper allows one to answer quantitatively questions such as “What is the degree of square-planarity content (or  $D_{4h}$ -ness,  $S(D_{4h})$ , as defined below), and what is the tetrahedrality content ( $S(T_d)$ ) in an  $AB_4$  molecule?”.

A tetracoordinated species constructed at random is characterized by a certain tetrahedrality content,  $S(T_d)$ , and by a certain planarity content,  $S(D_{4h})$ . As shown in Figure 1 for 10 000 randomly created tetrahedra,<sup>17</sup> many pairs of  $T_d$ -ness/ $D_{4h}$ -ness values are possible, filling up a whole cloud of dots. Also shown in Figure 1 is that even imposing restrictions, such as not allowing angles smaller than  $60^\circ$ , still leave a very broad band of structures with various tetrahedrality and planarity contents. One of the main findings reported here is that out of the large arsenal of tetrahedral structures allowed by pure geometry, copper complexes concentrate in an extremely narrow zone: Only very specific pairs of  $T_d$ -ness/ $D_{4h}$ -ness values that dictate

each the other are allowed, and these structures follow *strictly* the line superimposed in Figure 1. Hints that this line has some features of universality were provided by the analysis of Ni and Pt complexes, of metalloproteins, and even of covalent  $CC_4$  fragments.

First, we briefly recall how the symmetry content can be measured and what the special features of that measure are.

**Symmetry Measure: A Global Shape Descriptor.** The continuous symmetry measure (CSM) assesses quantitatively the degree of any symmetry within any structure. The algorithms,<sup>18</sup> computational details,<sup>19</sup> mathematical proofs,<sup>20</sup> and the applicability of the measure to many symmetry/chirality issues in chemistry (cited above) and beyond<sup>11</sup> were the topics of previous publications. We limit ourselves here only to some central points needed for this report. In general the CSM identifies the minimal distance of a given structure to a structure having the desired symmetry. It is a special distance function in that the specific coordinates of the nearest symmetric structure are not known a priori but are searched. Thus, given a (distorted) structure composed of  $N$  vertexes (the ligands and the central atom), the coordinates of which are  $\{Q_k, k = 1, 2, \dots, N\}$ , one searches for the vertex coordinates of the nearest perfectly  $G$ -symmetric object ( $G$  being a specific symmetry group),  $\{\hat{P}_k, k = 1, 2, \dots, N\}$ . Once at hand, the symmetry measure is defined as

$$S(G) = \min \frac{\sum_{k=1}^N |Q_k - \hat{P}_k|^2}{\sum_{k=1}^N |Q_k - Q_0|^2} \times 100 \quad (1)$$

where  $Q_0$  is the coordinate vector of the center of mass of the investigated structure, the denominator is a mean square size normalization factor, and the factor of 100 is introduced for convenience. (Normalization over the number of atoms cancels out as it appears in both the nominator and denominator.) It was proven elsewhere<sup>18</sup> that the bounds are  $100 \geq S \geq 1$ . If a structure has the desired  $G$  symmetry,  $S(G) = 0$ , and the symmetry measure increases as it departs from  $G$  symmetry, reaching maximal value (not necessarily 100). All  $S(G)$  values, regardless of  $G$ , are on the same scale and therefore comparable. The main computational problem is to find the nearest structure that has the desired symmetry, namely, how to minimize eq 1 to get  $\{\hat{P}_k, k = 1, 2, \dots, N\}$ . Several methods, both general and problem-specific, have been constructed toward this goal.<sup>20,21</sup> We use here the method described in ref 21, which employs for the minimization procedure of eq 1 an input structure that has the desired symmetry but that is not of minimal distance to the distorted one. This *prototype symmetric structure*, the coordinates of which are  $\{P_{0k}, k = 1, 2, \dots, N\}$ , undergoes minimizations that transform it to the desired set of vertexes,  $\hat{P}_k$ , which is the closest to the distorted  $Q_k$ . It has been shown<sup>21</sup> that in terms of the prototype symmetric structure,  $P_{0k}$ , minimization of eq 1 leads to

$$S(G) = 100 \times \left[ 1 - \frac{\left( \sum_{k=1}^N P_{0k}^t \mathbf{R}^t Q_k \right)^2}{N \sum_{k=1}^N |Q_k|^2} \right] \quad (2)$$

Here,  $\mathbf{R}$  is a rotation ( $3 \times 3$ ) matrix (and the upper index,  $t$ ,

(12) Kanis, K. D.; Wong, J. C.; Marks, T. S.; Ratner, M. A.; Zbrodsky, H.; Keinan, S.; Avnir, D. *J. Phys. Chem.* **1995**, *99*, 11061–11066.

(13) Buch, V.; Gershgoren, E.; Hel-Or, H. Z.; Avnir, D. *Chem. Phys. Lett.* **1995**, *247*, 149–153.

(14) Pinto, Y.; Fowler, P. W.; Mitchell, D.; Avnir, D. *J. Phys. Chem. B* **1998**, *102*, 5776–5784.

(15) Keinan, S.; Avnir, D. *J. Am. Chem. Soc.* **1998**, *120*, 6152–6159.

(16) Keinan, S.; Avnir, D. *J. Am. Chem. Soc.* **2000**, *122*, 4378–4384.

(17) The 10 000 tetrahedra were created by randomly selecting four different angles, keeping all bond lengths equal to 1 (placing the central atom at the origin of Cartesian coordinates). The 2000 population limited to angles above  $60^\circ$  was created similarly. The total population of Figure 1 is 12 000 tetrahedra.

shows the transposition of the matrix or vector). The set of minimized  $\{P_{0k}, k = 1, 2, \dots, N\}$ , namely,  $\hat{P}_k$ , provides the actual structure of the nearest symmetric structure.

We emphasize that  $S(G)$  is a global descriptor that takes into account all angles and bond lengths; in this sense it is quite different from structural deviation analyses that select a specific geometrical feature. We recall that for an  $n$ -vertexes molecule there are  $3n - 6$  degrees of freedom (9 for our  $AB_4$  structures), i.e.,  $3n - 6$  independent structural parameters, and therefore, not taking all into account may amount to the overlooking of some important contributions to the overall distortion. Furthermore, if one wishes to compare different families of molecules, only global descriptors can be used. Consider for instance the families of  $CuCl_4^{2-}$  and  $CC_4$  for which the average bond lengths are around 2.3 and 1.5 Å, respectively; the comparison of the symmetries of these two different systems is straightforward with the CSM methodology. Changes in specific geometric descriptors of course show up in the  $S(G)$  values, and the correlation between local and CSM descriptors was analyzed in detail by Alvarez and Llunell.<sup>22</sup>

## 2. Technical and Computational Details

**Structural Data Sources.** All structures were obtained from the Cambridge Structural Database (CSD) version 5.17, April 1999<sup>23</sup> and have  $R$  values less than 10%. All are listed in the Supporting Information, which details the following. For  $CuCl_4^{2-}$ , the CSD database was searched for all structures containing the discrete anion  $CuCl_4^{2-}$ . There are 114 files containing 131 structures of the anion, differing from each other by the counteraction, which were used. For  $CuBr_4^{2-}$ , the CSD contains 44 discrete structures of the anion, which were used in this study. For  $Ni(\text{monodentate})_4$ , the CSD database contains 19 files with 20 discrete structures of the anion of  $NiCl_4^{2-}$  and 55  $[Ni(CN)_4]^{2-}$  anions. For additional Cu complexes, 16 copper complexes that were noted in the past to possess “irregular” structures were also taken from the CSD. For fenestranes, the CSD database yielded seven structures. For  $[Pt(\text{halogen})_4]^{2-}$ , the CSD database yielded 43 anions. For metalloproteins, zinc centers at carbonic anhydrase II were selected. All 10 files were taken from PDB<sup>24</sup> structures.

**$CuCl_4^{2-}$  Energy Surface.** For the creation of the potential-energy surface, 144 structures were taken. These were selected from a Figure 1 type map based on planarization routes leading from a perfect tetrahedron to a planar square, as described in section 4. For each of the structures, the total energy was calculated by the Hartree–Fock method, using the basic set LACVP\*++<sup>25</sup> as implanted in the 3.5 Jaguar program.<sup>26</sup> A special feature of the Jaguar program was used, which helps the convergence of transition metals by creating a better initial guess of the wave function, as describe in ref 27. For each structure the angles were fixed, but bond lengths were allowed to relax. Out of the 144 structures, for 124 structures the energy calculation converged. Nine structures below the line shown in Figure 1 were also analyzed.

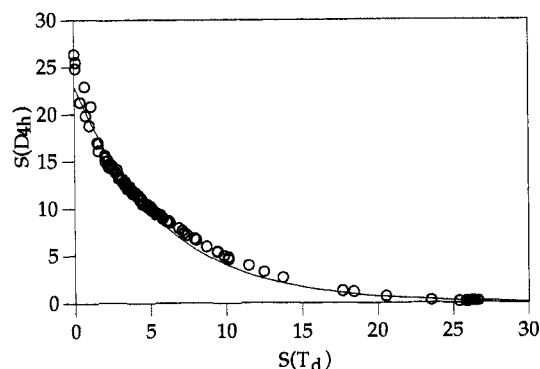


**Figure 2.** Correlation between planarity and tetrahedrity ( $S(D_{4h})$  vs  $S(T_d)$ ) for 131 discrete  $CuCl_4^{2-}$  anions. The line is an exponential fit (see text).

## 3. Observed Symmetry Correlations

Our starting point has been the family  $CuCl_4^{2-}$  complexes, which is one of the most studied anions in coordination chemistry.<sup>28</sup> As mentioned above, it appears in many geometries,<sup>6</sup> from square-planar to almost ideal tetrahedral,<sup>29</sup> spanning all the geometries in that range. We have analyzed the degree of tetrahedrity,  $S(T_d)$ , and the degree of square planarity,  $S(D_{4h})$ , of 131 discrete  $CuCl_4^{2-}$  structures and plotted these two symmetry measures against each other. As explained above, an unbiased a priori expectation would be to get a scatter of  $S(D_{4h})/S(T_d)$  pairs somewhere within the cloud shown in Figure 1. The actual result, shown in Figure 2 (compare with Figure 1) is of an extremely well-defined correlation line that collects all of the experimental  $S(D_{4h})/S(T_d)$  pairs to a specific, narrowly defined “path” of possible tetracoordinated structures leading from (almost) pure tetrahedrity (left side of the figure) to pure planarity (right side). Following Burgi and Dunitz’s proposition of “dynamics out of statics”,<sup>10</sup> we shall later remove the parentheses from “path”. The symmetries correlation line obeys a simple exponential equation,

$$S(D_{4h}) = a e^{-bS(T_d)} \quad (3)$$

with  $a = 22.91$  and  $b = 0.173$  (correlation fit,  $R^2 = 0.9855$ ). In this context it should be noted that nonlinear relations between structural parameters in copper complexes have been documented.<sup>9,30</sup>

The next step was to see if the symmetries correlation line of Figure 2 can represent a close family of complexes as well, namely, those of  $CuBr_4^{2-}$ . These complexes are also known to appear in many geometries and resemble  $CuCl_4^{2-}$  complexes in many of their properties.<sup>31</sup> The results for the 44 discrete anions found in the CSD are shown in Figure 3a, superimposed on the  $CuCl_4^{2-}$  trend, and it is seen that, indeed,  $CuBr_4^{2-}$  follows a very similar  $S(D_{4h})/S(T_d)$  symmetry behavior. Now it was interesting to see what happens if copper is replaced by another transition metal, and  $Ni(\text{monodentate})_4$  was selected for that purpose. The results for the 75 discrete anions ( $NiCl_4^{2-}$  and  $Ni(CN)_4^{2-}$ ) are shown in Figure 3b, again superimposed on the  $CuCl_4^{2-}$  trend, and again, it is seen that the two families of complexes follow a very similar trend.

- (18) Zabrodsky, H.; Peleg, S.; Avnir, D. *J. Am. Chem. Soc.* **1992**, *114*, 7843–7851.  
 (19) (a) Zabrodsky, H.; Peleg, S.; Avnir, D. *J. Am. Chem. Soc.* **1993**, *115*, 8278–8289. (b) Zabrodsky, H.; Peleg, S.; Avnir, D. *J. Am. Chem. Soc.* **1995**, *117*, 462–473.  
 (20) Salomon, Y.; Avnir, D. *J. Comput. Chem.* **1999**, *20*, 772–780.  
 (21) Pinsky, M.; Avnir, D. *Inorg. Chem.* **1998**, *37*, 5575–5582.  
 (22) Alvarez, S.; Llunell, M. *J. Chem. Soc., Dalton Trans* **2000**, *19*, 3288–3303.  
 (23) CSD 5.17, Cambridge Crystallographic Data Center, 12 Union Road, Cambridge, CB2 IEZ, U.K., April 1999.  
 (24) Bernstein, F. C.; Koetzle, T. F.; Williams, G. J. B.; Meyer, E. R. J.; Brice, M. D.; Rodgers, J. R.; Kennard, O.; Shimanouchi, T.; Tasumi, M. *J. Mol. Biol.* **1977**, *112*, 535–542.  
 (25) Hay, P. J.; Wadt, W. R. *J. Chem. Phys.* **1985**, *82*, 299–310.  
 (26) Jaguar, version 3.5; Schrodinger, Inc.: Portland, OR, 1997.  
 (27) Vacek, G.; Perry, J. K.; Langlois, J. M. *Chem. Phys. Lett.* **1999**, *310*, 189–194.

- (28) Smith, D. W. *Coord. Chem. Rev.* **1976**, *21*, 93–158.  
 (29) Exact tetrahedrity is not possible because of Jahn–Teller distortion (Jahn, H. A.; Teller, E. *Proc. R. Soc. London* **1937**, *A161*, 220–225.).  
 (30) Gazo, J.; Bersuker, I. B.; Garaj, J.; Kabesova, M.; Kohout, J.; Langfelderova, H.; Melnik, M.; Serator, M.; Valach, F. *Coord. Chem. Rev.* **1976**, *19*, 253–297.  
 (31) Hathaway, B. J.; Billing, D. E. *Coord. Chem. Rev.* **1969**, 143–207.

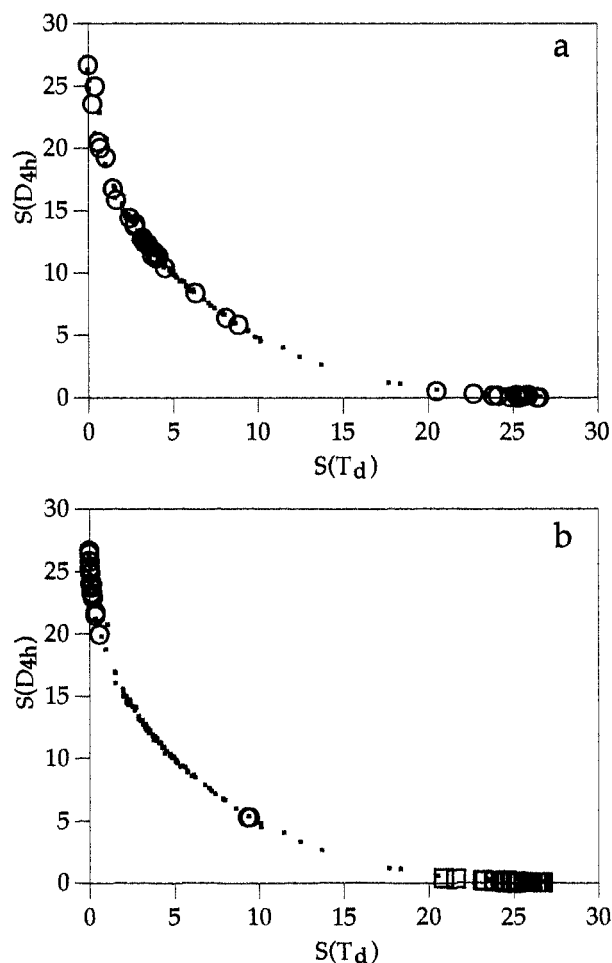


**Figure 3.**  $S(D_{4h})$  vs  $S(T_d)$  for (a)  $\text{CuBr}_4^{2-}$  anions (circles) and (b)  $\text{NiCl}_4^{2-}$  (circles) and  $\text{Ni}(\text{CN})_4^{2-}$  (squares), superimposed on the  $\text{CuCl}_4^{2-}$  data (small dots).

It was important for the establishment of the authenticity of the  $S(D_{4h})/S(T_d)$  correlation line to search for cases where the correlation line fails. For that purpose we returned to the copper complexes and analyzed additional structures, in particular those that were reported as having irregular cupric structures. Within this group of 16 structures (see Supporting Information) two were detected *not* to obey the general line (Figure 4a), and the shown structures<sup>32</sup> and their deviations are discussed below.

Most of the  $\text{AB}_4$  families do not assume all possible structures between tetrahedrality and planarity as Cu and Ni complexes do but tend to concentrate near one of these two symmetries. For instance, tetracoordinated Zn as well as  $\text{sp}^3$  carbon are, at most, distorted tetrahedra, while platinum complexes, on the other hand, are mainly square planar. It was interesting to see how these structures relate to the  $\text{CuCl}_4^{2-}$  line. Figure 4b shows that indeed the 43  $[\text{Pt}(\text{halogen})_4]^{2-}$  complexes coincide with the planar tail of the  $\text{CuCl}_4^{2-}$  line as perhaps would be expected. Less obvious, however, is the coincidence of seven  $\text{CC}_4$  fragments, taken from the center moieties of fenestranes<sup>33</sup> with this line. Interest in fenestranes has been part of the ongoing search for the still elusive nearly planar  $\text{sp}^3$  carbon.<sup>34</sup> The partial

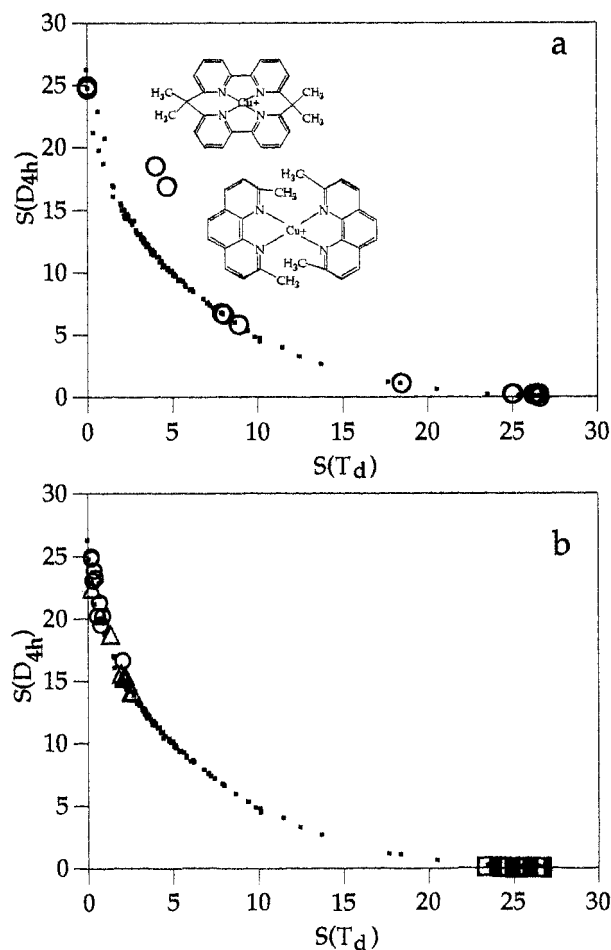


**Figure 4.**  $S(D_{4h})$  vs  $S(T_d)$  for (a) 16 copper complexes (which were described to possess “irregular” structures (circles), where two structures (shown) deviating from the correlation line structures are shown, and (b)  $\text{CC}_4$  centers in fenestranes (triangles),  $[\text{Pt}(\text{halogen})_4]^{2-}$  centers (squares), and Zn centers within carbonic anhydrase (circles). All are superimposed on the  $\text{CuCl}_4^{2-}$  data (small dots).

planarization of the  $\text{sp}^3$  carbon is made possible by fusing the central carbon atom with alkane rings. The fact that two completely different species, the organic, covalent bonded  $\text{CC}_4$  fragment and the inorganic coordinated anion  $\text{CuCl}_4^{2-}$ , are describable by the same symmetry change line indicates a possible generality of this specific tetrahedral–planar path. Indeed, compatible with the possibility of universality is the nonobvious case of 10 different Zn species within carbonic anhydrase II (ligated to three nitrogens from histidine residues and to the enzyme’s substrate), which follow the same  $S(D_{4h})/S(T_d)$  correlation line (Figure 4b). The encasing huge protein has sufficient mechanical force to impose a distorted geometry on the metal cation ligands, which is relevant for the catalytic action, and yet, it has selected the same distortive mode that is similar to the one imposed by crystal packing of small tetracoordinated molecules.

So, does the  $S(D_{4h})/S(T_d)$  symmetries correlation line have elements of universality? The collection of all data points for all of the structures of Figures 2–4 into one presentation is shown in Figure 5. It is seen that in general these complexes obey a general  $S(D_{4h})/S(T_d)$  symmetry behavior<sup>35</sup> characterized by eq 3 with parameters values ( $a = 25.32$ ,  $b = 0.199$ ,  $R^2 = 0.979$ ) close to those found for  $\text{CuCl}_4^{2-}$ . It is remarkable to see that the outcome of different forces that induce distortion (crystal packing, protein folding, Jahn–Teller effects, intramolecular forces) is funneled to the same coordinates of the  $S(D_{4h})/S(T_d)$

(32) MPYRCU (lower point) (bis(6,6'-dimethyl-2,2'-bipyridyl)copper tetrafluoroborate) and MPHCU (bis(2,9-dimethyl-1,10-phenanthroline)-copper nitrate dihydrate).

(33) Leuf, W.; Keese, R. *Adv. Strain Org. Chem.* **1993**, *3*, 229–267.

(34) (a) Hoffman, R.; Alder, R. W.; Wilcox, C. F., Jr. *J. Am. Chem. Soc.* **1970**, *92*, 4992–4993. (b) Rottger, D.; Erker, G. *Angew. Chem., Int. Ed. Engl.* **1997**, *36*, 812–827.

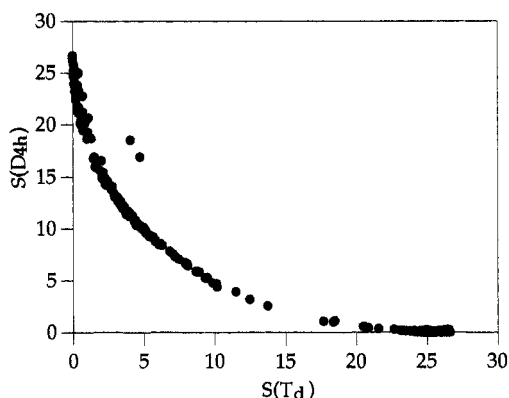


**Figure 5.**  $S(D_{4h})$  vs  $S(T_d)$  for all the above  $AB_4$  anions/centers. The symmetry behavior for many different species is seen to be quite similar.

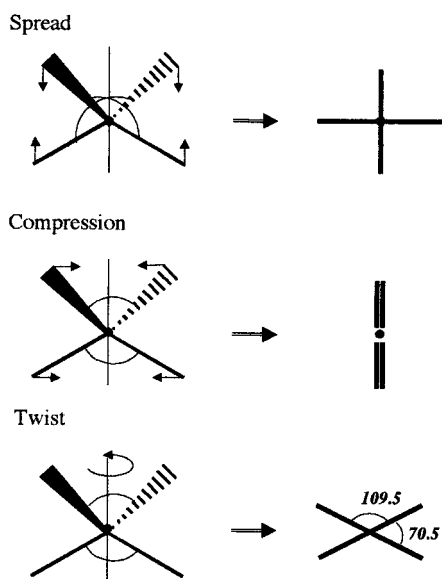


**Figure 6.** Three planarization routes of a tetrahedron: spread, where two opposite bond angles around the central ion spread out as shown by the arrows to yield a square-planar structure; compression, where two pairs of bonds are squeezed into an allenelike structure; and twist, where one pair of bonds is rotated into the plane of the other two bonds.

line and is *not* scattered within the general area of possible structures shown in Figure 1. In particular, it does not pass through the zones of high density of  $S(D_{4h})/S(T_d)$  points ( $S(T_d) \approx 15$ ,  $S(D_{4h}) \approx 13$  in Figure 1), which are geometrically the most probable tetrahedra for which no forces dictate the structure. In fact, *none* of the real structures we analyzed appears in the high-density area, but all follow very closely the lower limits of the  $S(D_{4h})/S(T_d)$  cloud of all possible tetrahedra.

#### 4. Data Analysis and Suggested Interpretations

Figure 5 indicates that there is a specific distortive mode that leads tetracoordinated structures from planarity to tetrahedrity. To search what this mode might be, we used the widely accepted categorization of tetrahedral planarization modes, namely, the spread, compression, and twist modes<sup>36</sup> (shown and explained in Figure 6), and analyzed their  $S(D_{4h})/S(T_d)$  symmetry-change behavior.<sup>37</sup> The results of the analysis, which was performed

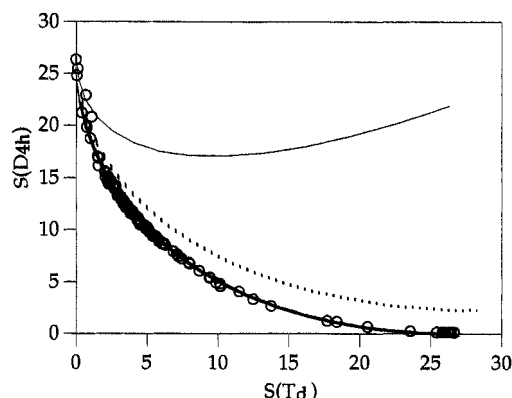


**Figure 7.**  $S(D_{4h})$  vs  $S(T_d)$  for the three planarization routes: compression (thin line), twist (dashed line), and spread (bottom black line). It is seen that the  $\text{CuCl}_4^{2-}$  anions (open circles) fit perfectly the spread line.

on 20 structures along each path, keeping equal bond lengths and two pairs of equal angles, are shown in Figure 7. The striking observation is that the spread mode (the  $B_{2u}$  vibrational mode<sup>38</sup>) perfectly fits the experimental  $\text{CuCl}_4^{2-}$   $S(D_{4h})/S(T_d)$  line and provides a good general fit for the other lines as well.

Is the fit coincidental or are the  $\text{CuCl}_4^{2-}$  structures along the line indeed spread-tetrahedral structures? To answer this question, we note that the spread distortion must keep one of the three dihedral angles at  $90^\circ$ ; sampling of structures from the line shows that this is the case. For instance, both  $\{[\text{bis}(2,6\text{-diamino-3,5-dichloropyridinium})\text{CuCl}_4]^{2-}$  (CSD code name, BEZGEZ) and  $\{[(3\text{-picoliniumylammonium})\text{CuCl}_4]^{2-}$  (NEFWIE) have an exact dihedral angle of  $90.0^\circ$ . Indeed the two structures that deviate from the spread line<sup>32</sup> (Figure 4a), have dihedral angles of  $99.0^\circ$  and  $94.7^\circ$ . This is due, probably, to the bicyclic strain causing both not to follow the spread path. Although the spread model is simple (equal bond lengths and angle pairs), its symmetry analysis does represent the real  $\text{CuCl}_4^{2-}$  structures, most of which are actually characterized by unequal bond lengths and/or angle sizes.<sup>39</sup> Such inhomogeneities in bond lengths and angles within the same tetracoordinated species are quite common for other structures in the combined line (Figure 5), but these structural properties come under the same umbrella in the symmetry analysis because of its unique feature of globality, namely, of treating the molecule as a whole. The nature of the symmetry measure is therefore distinctly different from analyses of distortions that are based on the changes of a specific geometrical parameter.<sup>40</sup>

Next we ask whether the spread correlation line represents the minimal geometrically distortive mode (i.e., the minimal  $S(D_{4h})/S(T_d)$  pair values). We return for this purpose to Figure 1. The superimposed line there is the spread line, and it is seen that although it passes very close to the lower values edge of the total cloud of the  $S(D_{4h})/S(T_d)$  pair values, there are structures that are somewhat lower. These structures are still very similar to spread structures but with one pair of bonds slightly tilted toward the other pair. Not yet having at hand a combined description of these somewhat less distorted structures, we remain with the straightforward spread model, having in mind that this model represents a large volume of experimental data quite closely.

(35) In addition, 118  $\text{PO}_4$  centers and 156  $\text{SiO}_3\text{R}$  fragments, all of which are very close to tetrahedrity ( $S(T_d) < 0.6$ ), sit close to this line as well but are not included for reasons described in section 4 (ref 44).

(36) Leuf, W.; Keese, R. *J. Mol. Struct.: THEOCHEM* **1992**, *257*, 353–368.

(37) Walden-type inversion, passing through a plane, was analyzed elsewhere.<sup>18</sup>

(38) Nakamoto, K. *Infrared and Raman Spectra of Inorganic and Coordination Compounds*; John Wiley and Sons: New York, 1986.

(39) For instance, for BEZGEZ and NEFWIE, the difference in bond lengths is 0.1 Å and bond angles differ by as much as  $2^\circ$ .

(40) Baur, W. H. *Acta Crystallogr.* **1974**, *B30*, 1195–1215.

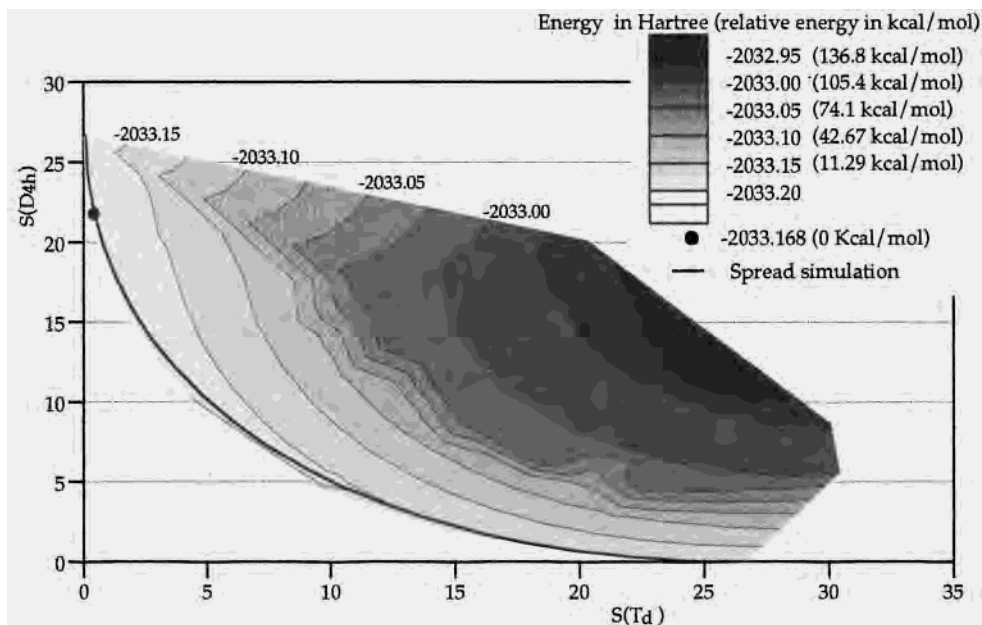


**Figure 8.** Potential energy/symmetry surface of  $\text{CuCl}_4^{2-}$ . The spread path is the black line. The global minimum is indicated by a black dot.

Since each of the structures on the symmetry correlation line resides in its own crystal-phase potential energy surface minimum, this line also represents a collection of minima of many potential energy surfaces. Some insight as to the possible trend of behavior of the collection of these minima may be obtained from comparison with the results of the analysis of the energy profile of the isolated molecule. Returning then to the  $\text{CuCl}_4^{2-}$  series, we first calculated the potential energies of various distorted (isolated)  $\text{CuCl}_4^{2-}$  structures<sup>41</sup> and plotted the resulting  $S(D_{4h})/S(T_d)$  symmetry/energy surface (Figure 8). This novel type of a potential energy surface shows that the *spread structures* (along the bold line) *comprise an energy minimum*.<sup>42</sup> This observation is in agreement with Murray-Rust et al.,<sup>10</sup> who suggested that “a distribution of sample points corresponding to observed structures will tend to be concentrated in low-lying regions of the potential energy surface”. It is also seen that the energy content along this line increases gradually from a nearly tetrahedral  $\text{CuCl}_4^{2-}$  global minimum structure (according to Hessian analysis) indicated as a black dot in Figure 8 ( $S(T_d) = 0.36$ ,  $S(D_{4h}) = 21.72$ ). This  $D_{2d}$ -symmetric structure is more stable than the  $D_{4h}$  planar structure by 15.2 kcal/mol. Similar energy differences were also found in other calculations of this system.<sup>43</sup> The energy rises on both sides of this minimum-energy valley, more shallowly at the tetrahedral end.<sup>44</sup> Thus, we have

(41) The structures were created by using the geometries of the spread and compression paths as limits (Figure 7), filling the gap between the two paths with minimal movements structures. For example, from the 9th structure (out of 20) in the spread path to the 9th structure (out of 20) in the compression path, 6 gradually changing structures were created.

(42) The small population of points that spills in Figure 1 below the spread line is of higher energy than the energy of the spread structures.

(43) The first energy calculation of  $\text{CuCl}_4^{2-}$  was done by Lohr and Lipscomb (Lohr, L. L.; Lipscomb, W. N. *Inorg. Chem.* **1963**, *2* (5), 912–917), with an energy difference between minimal and the square-planar structure of 30 kcal/mol. Additional calculations were made by Demuyneck et al. (Demuyneck, J.; Veillard, A.; Wahlgren, U. *J. Am. Chem. Soc.* **1973**, *95*, 5563–5569), who found 20 kcal/mol for this difference, and by Westbrook and Krogh-Jespersen (Westbrook, J. D.; Krogh-Jespersen, K. *Int. J. Quantum Chem.* **1988**, *22*, 245–255), who found 15.5–18.2 kcal/mol, depending on the basis set.

(44) It is apparently this energy shallowness and the fact that all three paths (Figure 7) merge near the tetrahedral end that result in a scatter among the three very closely lying paths (seen at a very high-resolution analysis) of the  $\text{PO}_4$  centers and 156  $\text{SiO}_3\text{R}_3$  fragments.

found that a valley of low symmetry pair values coincides with a valley of minimal energy for the isolated  $\text{CuCl}_4^{2-}$ . In other words, we found that *molecular symmetry distortions follow a (nearly) minimal geometric motion that allows it along a minimal energy route*. Although the energy calculations are for an isolated species, leading to somewhat less compact structures than in crystal packing, we propose, with all known reservations for such comparisons, that this result is indicative of the tetracoordinated structures of Figure 5 as well, at least on the level of a general trend.

## 5. Conclusion

We have shown that quantitative symmetry analysis is capable of identifying new types of structural correlations and of quantifying the relation between energy and symmetry. The result that many different and unrelated tetracoordinated species, inorganic, organic, and bioinorganic, tend to select very similar distortive modes is, in our view, remarkable. Comparison of different chemical species is made possible because of the globality of the symmetry measure, which analyzes the shape of a molecule as a whole. The intimate quantitative correlation between energy and symmetry, already demonstrated for chiral fullerenes enantiomerizations<sup>14</sup> and for the binding of HIV  $C_2$  inhibitors,<sup>16</sup> is further strengthened in this report in a more general way. Symmetry analyses of other coordination-number compounds is in progress. Correlations between symmetry properties of tetracoordinated complexes and their spectral properties have been identified and will be published separately.

**Acknowledgment.** This work is supported by the U.S.–Israel Binational Science Foundation. We thank Prof. K. Lipkowitz for in-depth, useful correspondence on various issues of symmetry/chirality measures from which this report gained a lot. We thank Dr. Mark Pinsky and Dr. M. Llundell for useful programming and computational support and Prof. S. Alvarez for helpful discussions and for carefully reading this manuscript and commenting on it.

**Supporting Information Available:** Listing of all compounds used in this study (CSD and PDB codes) as well as their  $S(T_d)$  and  $S(D_{4h})$  values. This material is available free of charge via the Internet at <http://pubs.acs.org>.